

Optimisation of Mo doping to form NiCoMo ternary sulphides for high performance charge storage.

a. School of Materials Science and Engineering, Nanchang University, Nanchang
330031, China

Figure Captions

Fig. S1. SEM images of (a) N_1C_1 , (b) N_1C_2 , (c) $N_2C_1S_{0.05}$, (d) $N_2C_1S_{0.08}$, (e) $N_2C_1S_{0.1}$ and (f) $N_2C_1S_{0.3}$

Fig. S2. SEM image of $Ni_2Co_1MS_{0.2-2}$ electrode after cycling.

Fig. S3. (a) XPS full spectrum of after cycling test; (b), (c), (d), (e) and (f) spectra of Ni, Co, Mo, S and O, respectively.

Fig. S4. XRD plots of $N_2C_1MS_{0.2-2}$ electrodes after cycling.

Fig. S5. (a) and (b) show the CV and GCD curves of N_1C_1 , N_1C_2 and N_2C_1 electrodes at $5\text{ mV}\cdot\text{s}^{-1}$ scan rate and $1\text{ A}\cdot\text{g}^{-1}$ current density; (c) and (d) show the CV and GCD curves of nickel-cobalt sulphide electrodes prepared with different sulphur additions at $5\text{ mV}\cdot\text{s}^{-1}$ scan rate and $1\text{ A}\cdot\text{g}^{-1}$ current density.

Fig. S6. (a) CV curves of the N_2C_1 electrode at different scan rates and (b) GCD curves at different current densities.

Fig. S7. (a) CV curves of the $N_2C_1S_{0.2}$ electrode at different scan rates and (b) GCD curves at different current densities.

Fig. S8. (a) CV curves of the $N_2C_1MS_{0.2-1}$ electrode at different scan rates and (b) GCD curves at different current densities.

Fig. S9. (a) CV curves of the $N_2C_1MS_{0.2-3}$ electrode at different scan rates and (b) GCD curves at different current densities.

Fig. S10. Cycle performance graph of $N_2C_1MS_{0.2-2}$ electrode.

Fig. S11. CV curves of $N_2C_1MS_{0.2-2}$ electrode and AC at $10\text{ mV}\cdot\text{s}^{-1}$ scan rate.

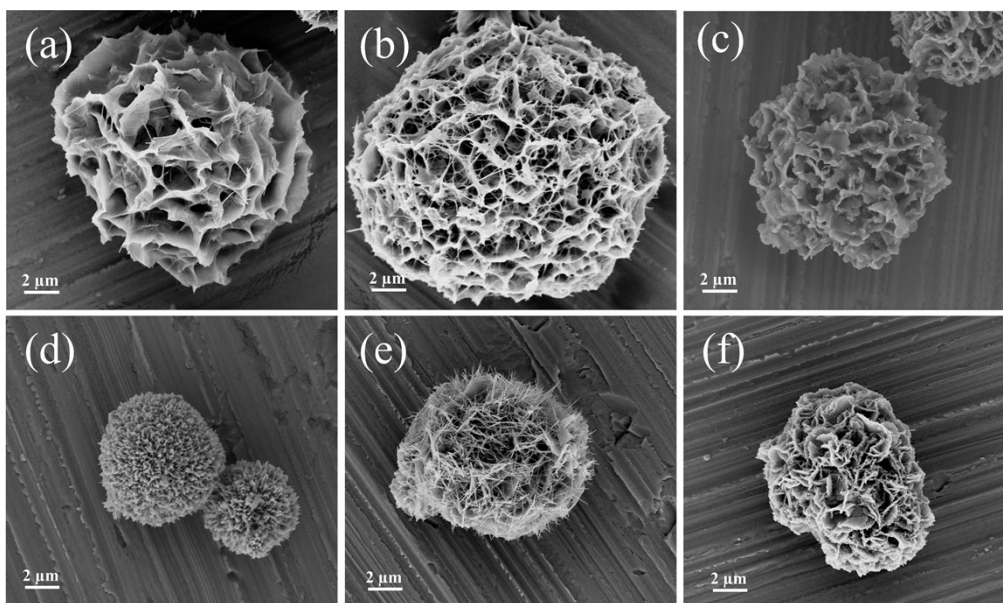


Fig. S1. SEM images of (a) N_1C_1 , (b) N_1C_2 , (c) $N_2C_1S_{0.05}$, (d) $N_2C_1S_{0.08}$, (e) $N_2C_1S_{0.1}$ and (f) $N_2C_1S_{0.3}$

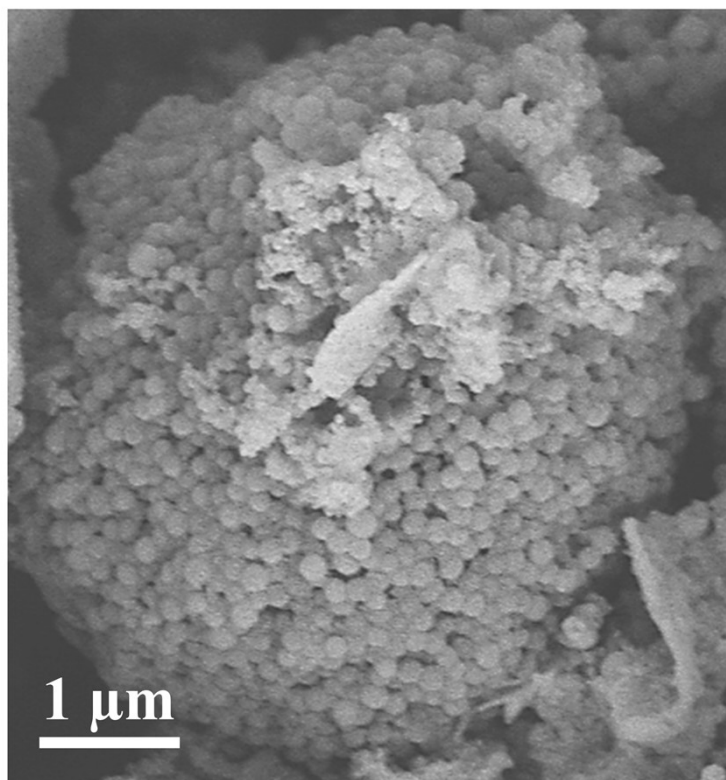


Fig. S2. SEM image of Ni₂Co₁MS_{0.2-2} electrode after cycling.

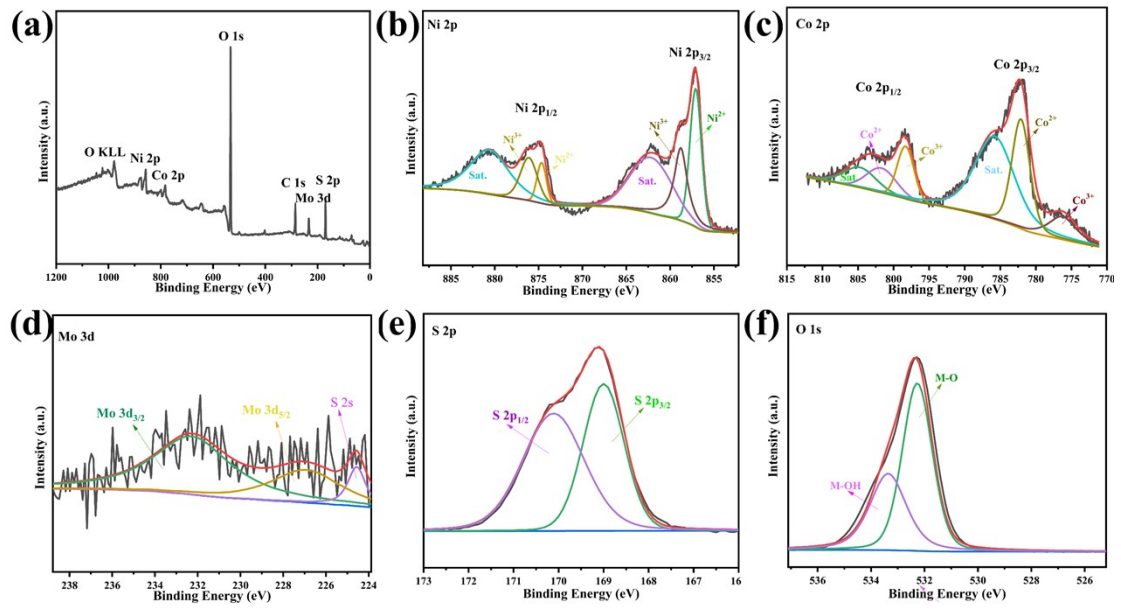


Fig. S3. (a) XPS full spectrum of after cycling test; (b), (c), (d), (e) and (f) spectra of Ni, Co, Mo, S and O, respectively.

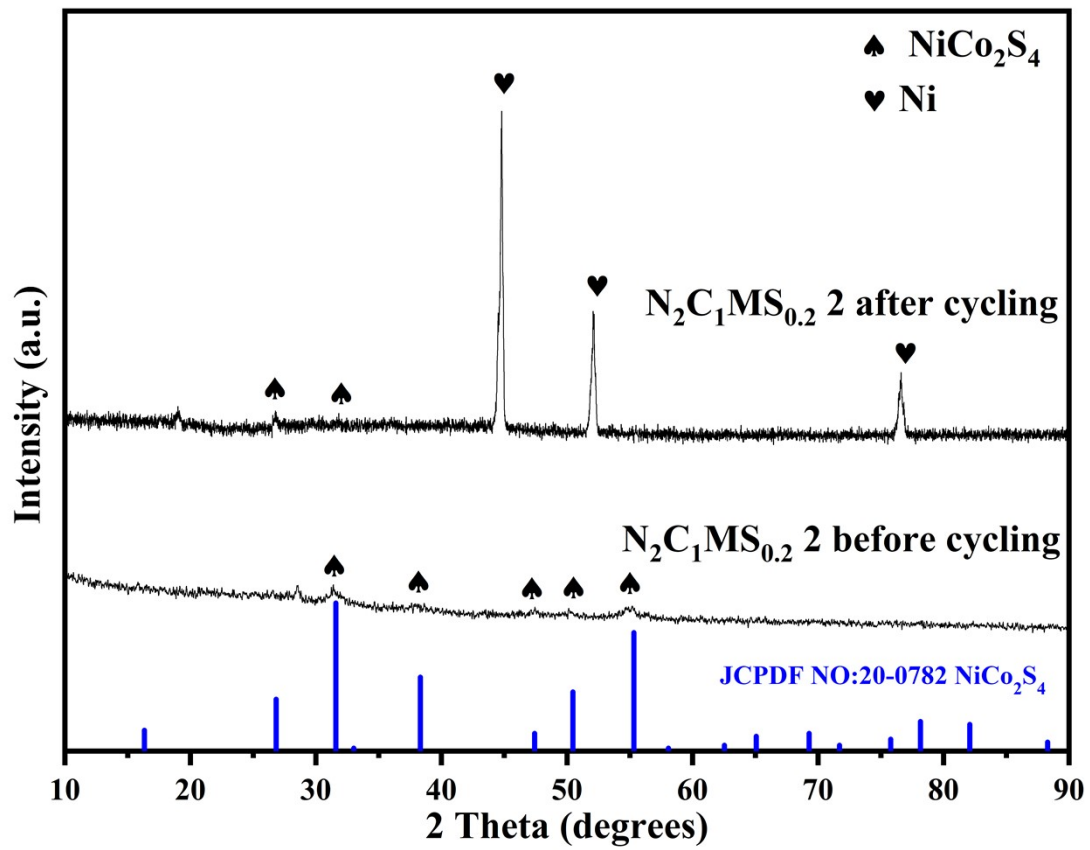


Fig. S4. Full XPS spectra after cycling of $N_2C_1MS_{0.2} 2$ electrodes.

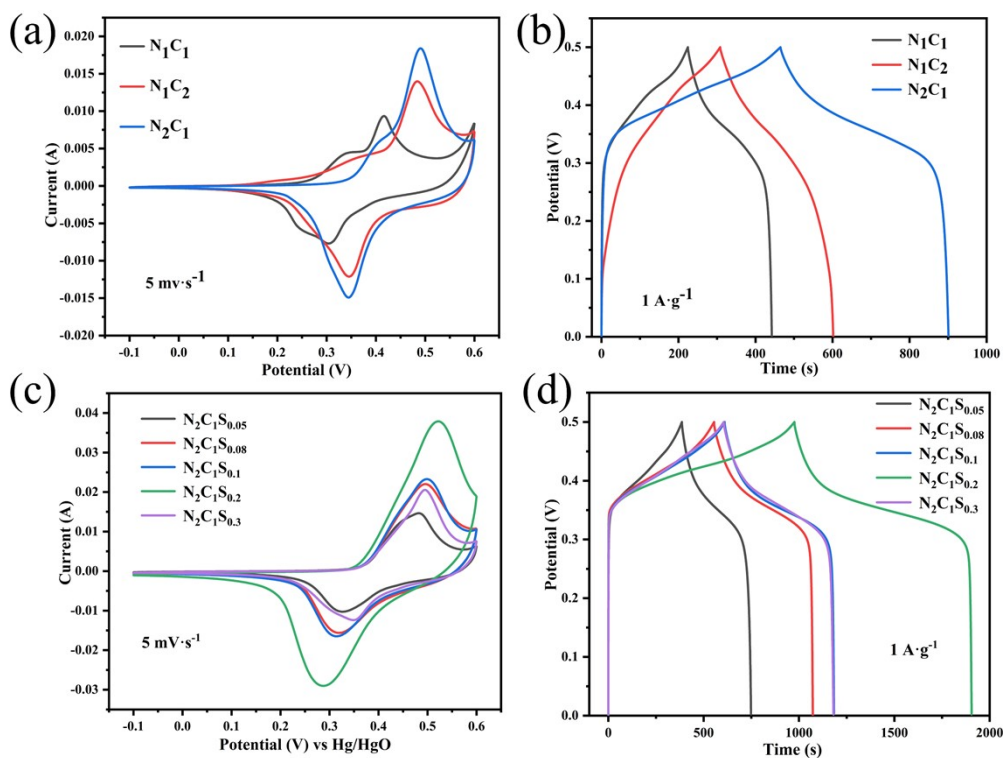


Fig. S5. (a) and (b) show the CV and GCD curves of N_1C_1 , N_1C_2 and N_2C_1 electrodes at $5 \text{ mV}\cdot\text{s}^{-1}$ scan rate and $1 \text{ A}\cdot\text{g}^{-1}$ current density; (c) and (d) show the CV and GCD curves of nickel-cobalt sulphide electrodes prepared with different sulphur additions at $5 \text{ mV}\cdot\text{s}^{-1}$ scan rate and $1 \text{ A}\cdot\text{g}^{-1}$ current density.

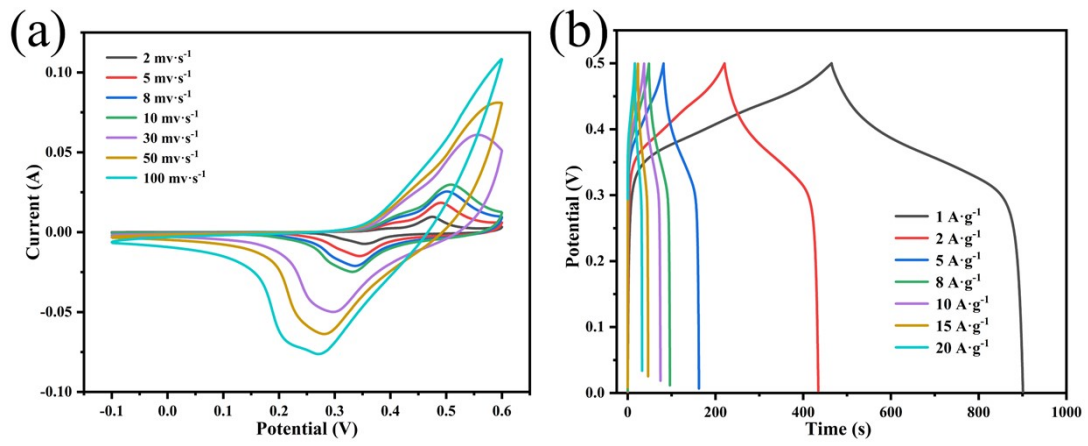


Fig. S6. (a) CV curves of the N_2C_1 electrode at different scan rates and (b) GCD curves at different current densities.

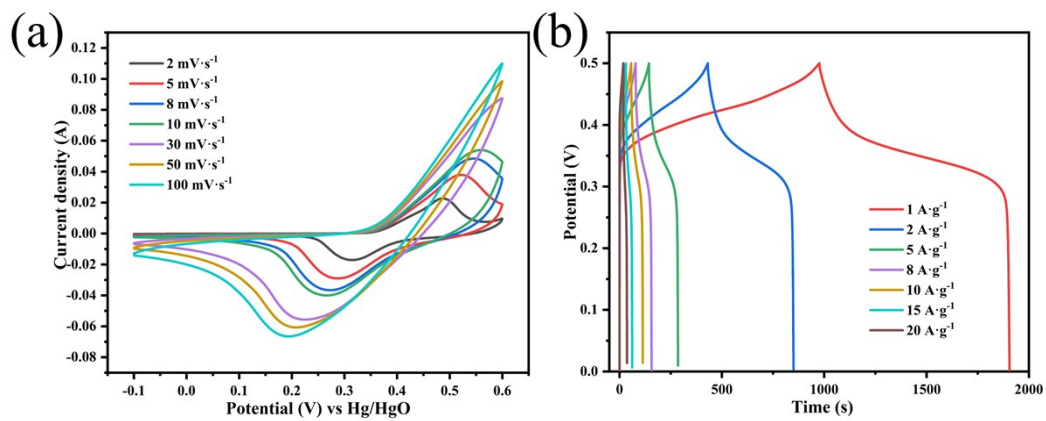


Fig. S7. (a) CV curves of the $N_2C_1S_{0.2}$ electrode at different scan rates and (b) GCD curves at different current densities.

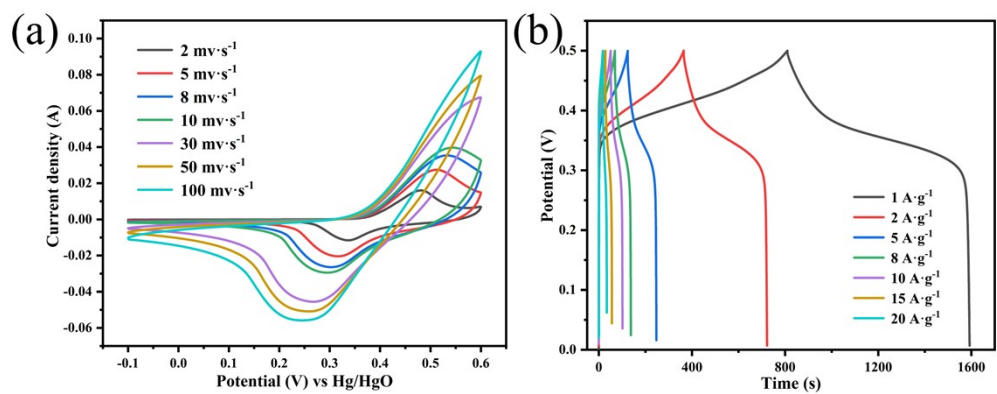


Fig. S8. (a) CV curves of the $N_2C_1MS_{0.2-1}$ electrode at different scan rates and (b) GCD curves at different current densities.

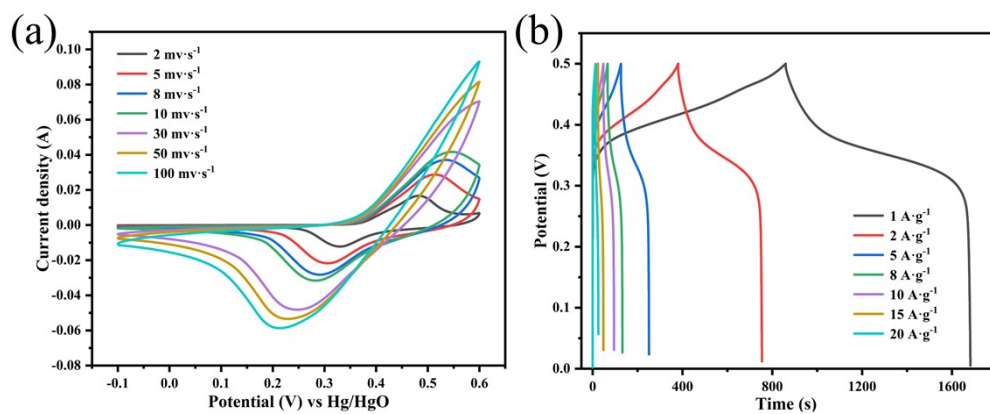


Fig. S9. (a) CV curves of the $N_2C_1MS_{0.2-3}$ electrode at different scan rates and (b) GCD curves at different current densities.

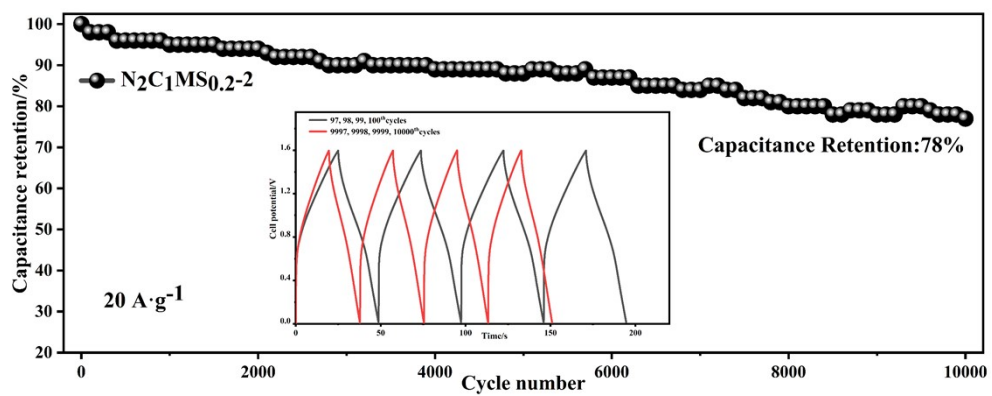


Fig. S10. Cycle performance graph of $N_2C_1MS_{0.2-2}$ electrode.

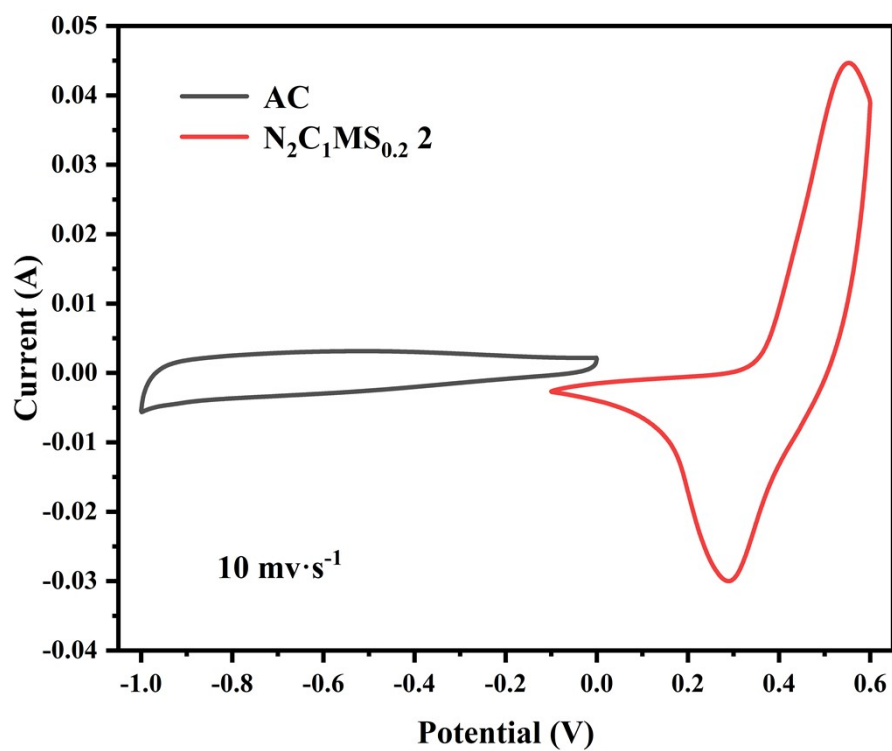


Fig. S11. CV curves of N₂C₁MS_{0.2}-2 electrode and AC at 10 mV·s⁻¹ scan rate.